International Journal of
High-Rise Buildings
www.ctbuh-korea.org/ijhrb/index.php

*International Journal of High-Rise Buildings*
*December 2022, Vol 11, No 4, 331-346*
*https://doi.org/10.21022/IJHRB.2022.11.4.331*

# Inflow Conditions for Modelling the Neutral Equilibrium ABL Based on Standard k-ε Model

**Jinghan Wang[1], Chao Li[1†], Yiqing Xiao[1], and Jinping ou[1]**

*Harbin Institute of Technology, Shenzhen, Shenzhen, 518055, China*

**Abstract** Reproducing the horizontally homogeneous atmospheric boundary layer in computational wind engineering is essential for predicting the wind loads on structures. One of the important issues is to use fully developed inflow conditions, which will lead to the consistence problem between inflow condition and internal roughness. Thus, by analyzing the previous results of computational fluid dynamic modeling turbulent horizontally homogeneous atmospheric boundary layer, we modify the past hypotheses, detailly derive a new type of inflow condition for standard k-ε turbulence model. A group of remedial approaches including formulation for wall shear stress and fixing the values of turbulent kinetic energy and turbulent dissipation rate in first wall adjacent layer cells, are also derived to realize the consistence of inflow condition and internal roughness. By combing the approaches with four different sets of inflow conditions, the well-maintained atmospheric boundary layer flow verifies the feasibility and capability of the proposed inflow conditions and remedial approaches.

**Keywords** Enhanced wall treatment, Inflow conditions, Neutral atmospheric boundary layer, Standard k-ε turbulence model, Wall shear stress.

†Corresponding author:
Chao Li
E-mail:
ichaosz@hit.edu.cn

## 1. Introduction

Since the atmospheric wind loading on buildings, bridges, and structures could be sophisticated, it is obliged to reproduce the wind flow field around these structures accurately. Thus, realizing the Horizontally Homogeneous Atmospheric Boundary Layer (HHABL) in Computational Wind Engineering (CWE) becomes one of the essential problems, which aims at keeping inflow wind properties unchanged along the longitudinal direction of an empty computational domain. Although the large eddy simulation (LES) is popular for current research on turbulent ABL, the Reynolds-Averaged Navier-Stokes equation (RANS) model is widely used in evaluating wind-induced loadings on structures(Yang et al., 2008; Longo et al., 2017), analyzing pollutant dispersion (Riddle et al., 2004; Yu and Thé, 2017), and commenting pedestrian wind environment (Blocken et al., 2007; 2016). Therefore, accurate wind flow properties are the most essential problem need to be solved. Scholars have done lots of work to obtain neutral equilibrium ABL.

Neutral stratified, equilibrium, horizontally homogeneous ABL means the streamwise gradients of flow properties are zeros through the domain. However, maintaining characteristics of inflow wind such as mean wind speed and turbulent kinetic energy (TKE) etc. implies the consistence of inflow conditions, boundary conditions, turbulence model and wall-functions (Sumner and Masson, 2012), which is complicated to implement.

One of the popular research points is proposing inflow conditions that includes mean velocity, turbulent kinetic energy and turbulent dissipation rate (TDR) profiles for k-ε turbulence closures, which usually accompanied by corresponding compensation measures. The inflow conditions can be divided into two types according to the distribution of TKE along ABL height, i.e., constant TKE and decreasing TKE.

The representative constant TKE profile is proposed by Richard and Hoxey (1993). The inflow conditions also contain logarithmic mean velocity and TDR profiles for standard k-ε turbulence model (Jones and Launder, 1972). This set of inflow conditions are extensively used and studied by later researchers and doubt are raised for reproducing the HHABL by using this inflow conditions. Then Richard and Norris (2011) emphasized the indispensability of implementing the suitable boundary conditions and wall treatment when reproducing the HHABL rather simply using the inflow conditions. Hargreaves and Wright (2007) reproduced HHABL based on this inflow conditions by modifying the wall-function and boundary

conditions. Besides, with regards to the boundary layer flow without shear stress at the top boundary of the domain, Richard et al. (2015) recommended an appropriate inflow condition for modelling equilibrium boundary layer flow. The inflow profiles are suitable for standard k-ε, Wilcox k-ω (Wilcox, 1998) and SST k-ω turbulence models and associated an appropriate rough wall treatment for the domain bottom boundary.

However, a shortcoming of this method is that the turbulent kinetic energy keeps unchanged along the vertical direction, which is not compatible with the profiles measured in wind tunnel test and physical atmospheric boundary layer that TKE decreased with height (Gorlé et al., 2009). Thus, Yang et al. (2009) proposed a new type of inflow conditions based on standard k-ε model including decreasing TKE along height. They verified its feasibility to numerical simulate HHABL by changing the turbulence model constants, which are determined from the wind tunnel data. Recently, Yang et al. (2017) extended this method into SST k-ω turbulence model and obtained two sets of equilibrium ABLs including logarithmic law and power law for mean velocity. The model constants were also changed.

Gorlé et al.(2009) simulated HHABL by using inflow conditions proposed by Yang et al (2009) and modified model constants, which were determined by wind tunnel test data. But they ignored the limitation that roughness constant $C_s \in [0,1]$ in Fluent, to satisfy the requirement that $k_s$ should be smaller than the height of first wall-adjacent layer, and changed the constants ($C_\mu$, $\sigma_\varepsilon$) of standard k-ε turbulence model. Then they applied this inflow condition to the study of dispersion in the wake of a blunt body.

Besides of the distribution of TKE profiles, the consistence between inflow conditions and ground roughness condition of computational domain is another important issue. Blocken et al (2007) analyzed the importance of modifying wall-functions for decreasing the streamwise gradients of simulated ABL detailed. Also, they recommended several remedial measures for realizing HHABL in standard k-ε turbulence model with standard wall functions (Launder and Spalding, 1974). In addition, they concluded four requirements for accurately descripting the flow near the ground surface, two most important requirements of which are high mesh resolution and a distance from the center point of the wall-adjacent cell to the wall $z_p$ should larger than the equivalent sand-grain roughness height $k_s$ of the terrain.

According to the remedial suggestions of Blocken (2007), Peralta et al.(2014) modified the standard wall functions when applying inflow profiles and boundary conditions of Richard and Hoxey (1993) into simulating ABL over complex terrain and obtained well performed results. O Sullivan et al. (2011) quantitatively analyzed the streamwise gradients in boundary layer flow which caused by the inconsistent top boundary conditions of the domain, derived consistent top boundary conditions for Richard's (1993) and Yang's (2009) inflow conditions and emphasized the significances of consistent top boundary conditions.

Based on standard k-ε turbulence model, Juretić and Kozmar (2013) proposed a novel approach by adjusting inlet pressure to realize the consistence between inflow profiles and wall boundary conditions, the model constants are changed meanwhile. Then, they extended this approach to various two-equation turbulence models, i.e., realizable k-ε, RNG k-ε and k-ω turbulence models (Juretić and Kozmar, 2014). Compared to the wind tunnel test data, the results of their work showed that k-ε models showed good homogeneity of mean velocity and TKE in most parts of the computational domain, while the simulation with k-ω model resulted a poor mean velocity in higher heights and better TKE profile.

Furthermore, some scholars dedicate effort to eliminate the streamwise gradients of flow properties by adding source terms into scalar transport equation. Parente et al. (2011a; 2011b) adding source terms to the TKE and TDR transport equations when using Yang's (Yang et al., 2009) and Richard's (Richards and Hoxey, 1993) inflow profiles in standard k-ε turbulence model, and re-defined the wall function constant and dimensional wall distance to improve the accuracy of k-ε turbulence model combined with standard wall function and to release the limitation for grid resolution in simulating HHABL. The results showed good homogeneity of the generated HHABL and the capability of this approach for simulating the flow around bluff-body was validated. Then Balogh et al.(2012) accomplished this approach in OpenFOAM and applied in simulation of flow over terrains with complex ground surface. Recently, Balogh and Parente (Balogh and Parente, 2015) extended the TKE profile into a four-parameter formulation and given the corresponding source terms. The simulation results showed better consistence to the wind tunnel experiments than Parente's work (Parente et al., 2011a). Hu et al. (2013) proposed a set of inflow conditions based on SST k-ω turbulence model and derived source term for TKE and specific dissipation rate and achieved an HHABL in empty domain. Cai et al. (2014) proposed a dynamic procedure with streamwise body force (driven force) within the whole boundary layer flow and obtained well performed equilibrium ABL. Besides, Yan et al. (2015) proposed a modelling procedure for inflow conditions that contains arbitrary shear stress models, which included source terms for TKE and TDR transport equations of standard k-ε turbulence model. The application of this method into wind flows over flat and complex terrains showed good homogeneity of the generated inflow conditions.

It can be concluded that most of the previous work involving modifications are usually modifying the turbulence model constants embedded in commercial CFD software. However, the model constants adopted in Fluent are

determined based on large number of experiences on studying turbulent shear flows and are widely acknowledged in simulating wall-bounded flows (Launder and Spalding, 1974; Hu et al., 2013). In addition, the model constants are closely related to each other, once change one of them others needed to be changed otherwise unreasonable phenomenon would occur. Thus, we will focus on the domain modification rather than correcting turbulence model in this paper.

The organization of this paper is as follows. In section 2, the hypotheses proposed by Richard and Hoxey (1993) will be given and advanced to propose a set of inflow conditions, two remedial approaches for reproducing HHABL will also be given. In section 3, numerical setups based on Fluent will be described in detail. In section 4, the validation results of new inflow conditions will be elaborated.

## 2. Inflow Conditions

### 2.1. Hypotheses in Equilibrium ABL Modelling

*2.1.1. Hypotheses proposed by Richard and Hoxey*

Most of the simulations for HHABL are based on RANS two-equation turbulence model, standard k-ε model and the respective transportation equations are

$$\frac{\partial(\rho u_i)}{\partial t}+\frac{\partial(\rho u_i u_j)}{\partial x_j}=-\frac{\partial p}{\partial x_i}+\frac{\partial}{\partial x_j}\left(\mu\frac{\partial u_i}{\partial x_j}-\rho\overline{u_i' u_j'}\right)+S_i \tag{1}$$

$$\frac{\partial(\rho k)}{\partial t}+\frac{\partial(\rho k u_i)}{\partial x_i}=\frac{\partial}{\partial x_j}\left[\left(\mu+\frac{\mu_t}{\sigma_k}\right)\frac{\partial k}{\partial x_j}\right]+G_k-\rho\varepsilon+S_k \tag{2}$$

$$\frac{\partial(\rho\varepsilon)}{\partial t}+\frac{\partial(\rho\varepsilon u_i)}{\partial x_i}=\frac{\partial}{\partial x_j}\left[\left(\mu+\frac{\mu_t}{\sigma_\varepsilon}\right)\frac{\partial\varepsilon}{\partial x_j}\right]+\frac{C_{1\varepsilon}\varepsilon}{k}G_k-C_{2\varepsilon}\rho\frac{\varepsilon^2}{k}+S_\varepsilon \tag{3}$$

where, $i=1, 2, 3$ represents streamwise, lateral and vertical direction for 3D flows. $k$ is turbulent kinetic energy, $\varepsilon$ is turbulent dissipation rate, $\rho$ is air density, $\mu_t$ is turbulent viscosity, $\mu$ is laminar eddy viscosity, $\sigma_k$, $\sigma_\varepsilon$, $C_{1\varepsilon}$, $C_{2\varepsilon}$ are model constants, $G_k=-\rho\overline{u_i' u_j'}\frac{\partial u_j}{\partial x_i}$ represents the generation of TKE due to the mean velocity gradients, $S_i$, $S_k$ and $S_\varepsilon$ are user defined source terms.

Based on standard k-ε turbulence model, Richards and Hoxey (1993)proposed a set of hypotheses and one type of inflow conditions including constant TKE along height and logarithmic mean velocity, which are listed in Table 1. The hypotheses are widely adopted in subsequent simulation and contains:

(1) The vertical velocity is zero: $w=0$;
(2) The pressure along vertical and streamwise directions are constants: $p=$ const.;
(3) The shear stress is constant: $\tau=$ const.

Besides, Yang et al. (2009) proposed a different inflow condition in which TKE decreases with height, which can be found in Table 1. In the following sections, we call the inflow condition proposed by Richards and Hoxey (1993) as "RH inflow condition" and Yang's (2009) inflow condition as "YY inflow condition".

*2.1.2. Modified hypotheses*

According to wind tunnel test, the tested turbulent flow can be regarded as 1D flow which is dominant by the wind flow in streamwise direction (Juretić and Kozmar, 2014). Thus, the simulations are implemented as 2D boundary layer flow in this paper to illustrating problems and economically evaluating possible remedial approaches. By introducing the Boussinesq hypotheses, the momentum conservation equation in streamwise direction ($\chi$) can be described as

$$\frac{\partial(\rho uu)}{\partial x}+\frac{\partial(\rho uw)}{\partial z}=-\frac{\partial p}{\partial x}+\frac{\partial}{\partial z}\left[(\mu+\mu_t)\frac{\partial u}{\partial z}\right] \tag{4}$$

In above equations, $u$ and $w$ are the mean velocity in streamwise and vertical directions respectively, $\tau=\mu_t\frac{\partial u}{\partial z}$ is the shear stress. Apparently, the gradient of horizontal velocity $u$ in turbulent HHABL satisfies $\frac{\partial(\rho uu)}{\partial x}=0$ and $w=0$ leads to $\frac{\partial(\rho uw)}{\partial z}=0$. Moreover, the turbulent and

**Table 1.** RH and YY inflow conditions

| Inflow Conditions | RH | YY |
|---|---|---|
| Mean Velocity | $u=\frac{u_*}{\kappa}\ln\left(\frac{z+z_0}{z_0}\right)$ | |
| TKE | $k=\frac{u_*^2}{\sqrt{C_\mu}}$ | $k=\frac{u_*^2}{\sqrt{C_\mu}}\sqrt{C_1\ln\left(\frac{z+z_0}{z_0}\right)+C_2}$ |
| TDR | $\varepsilon=\frac{u_*^3}{\kappa(z+z_0)}$ | $\varepsilon=\frac{u_*^3}{\kappa(z+z_0)}\sqrt{C_1\ln\left(\frac{z+z_0}{z_0}\right)+C_2}$ |

laminar viscosities satisfy $\mu_t \times \mu$ in highly turbulent flows. Thus, the momentum governing Eq. (4) can be simplified as

$$\frac{\partial p}{\partial x} = \frac{\partial \tau}{\partial z} = 0 \tag{5}$$

If the hypothesis (2) in section  is tenable, we will have the shear stress keeps constant through the boundary layer, i.e., hypothesis (3) is tenable. The magnitude of the retarding shear stress for the HHABL can be characterized by the friction velocity $u^*$, i.e., $\tau = \rho u^*$.

As listed in Table 1, RH and YY inflow conditions are based on the former hypotheses and the simplified momentum Eq.(5). After rebuilding the mesh of the barrier free computational domain employed in Yang et al.(2009) and imposing the two inflow conditions in ANSYS-Fluent, we found that obvious pressure gradient along the flow streamwise direction appeared and the pressure contours are shown in Figure 1.

After found this phenomenon, we compare the gradient of pressure in streamwise direction and shear stress gradient in vertical direction. The streamwise pressure at the middle of domain height ($z = 0.9$ m) and its fitted first-order polynomials can be seen in Figure 2, and the vertical sampled shear stress near the outlet ($x = 11$ m) and its fitted polynomials are also plotted in Figure 3. It can be seen that, a) the pressure is changing linearly along the streamwise direction despite a small variation in RH inflow condition, and b) the shear stress is not always constant in the vertical direction. Furthermore, it's worth noting that $\partial p/\partial x = -0.159$ and $\partial \tau/\partial z = -0.155$ are almost the same but not zero in YY inflow condition,

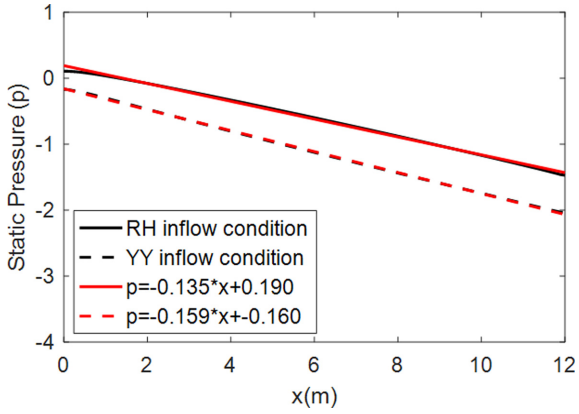



**Figure 2.** Streamwise pressure.

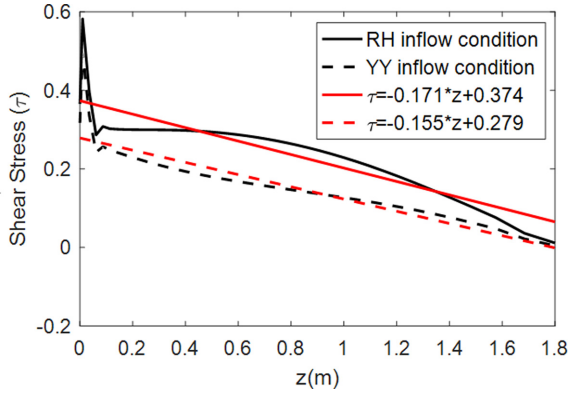



**Figure 3.** Vertical shear stress.

$\partial p/\partial x = -0.135$ and $\partial \tau/\partial z = -0.171$ are quite close but not zero in RH inflow condition either.

Thus, according to the findings above, the hypotheses

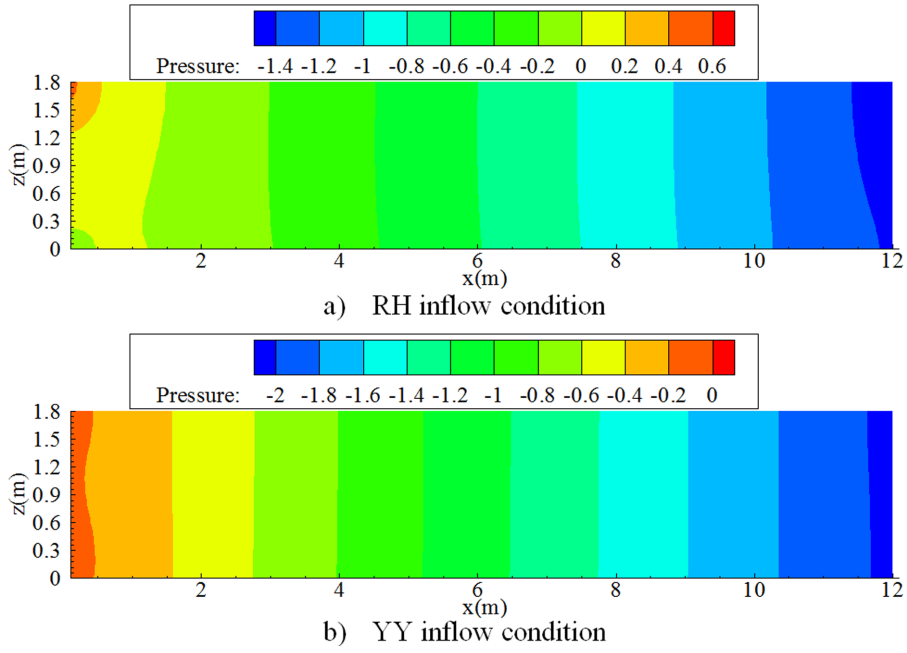



**Figure 1.** Pressure contour of the turbulent flow with different inflow conditions.

can be modified to wider applications:

(1) The vertical velocity is zero: $w = 0$;
(2) The pressure along vertical direction is constant: $\partial p/\partial z = 0$
(3) The pressure gradient in streamwise direction is constant: $\partial p/\partial x = \text{const}$
(4) The shear stress gradient in vertical direction is constant: $\partial \tau/\partial z = \text{const}$

### 2.2. New inflow conditions

Based on the modified hypotheses in previous section, the simplified momentum governing Eq.(5) should be rewritten as

$$\frac{\partial p}{\partial x} = \frac{\partial \tau}{\partial z} = \text{const.c} \tag{6}$$

The turbulent eddy viscosity in the standard k-ε turbulence model is defined as

$$\mu_t = \rho C_\mu \frac{k^2}{\varepsilon} \tag{7}$$

The production of TKE in standard k-ε turbulence model is evaluated by $G_k = -\rho\overline{u'w'}\frac{\partial u}{\partial x}$, combine with $\tau = \mu_t \frac{\partial u}{\partial z}$ and we obtain

$$G_k = -\rho\overline{u'w'}\frac{\partial u}{\partial z} = \tau\frac{\partial u}{\partial z} = \mu_t\left(\frac{\partial u}{\partial z}\right)^2 \tag{8}$$

The homogeneous turbulent flow can be considered in a local equilibrium state, which means the turbulence production is equal to the turbulence dissipation, i.e., $G_k = \rho\varepsilon$. Substitute this Eq. into Eq. (8) and combine with Eq. (7), we obtain the relationships below:

$$\varepsilon = \sqrt{C_\mu} k \frac{\partial u}{\partial z} \tag{9}$$

Substitute this Eq. into $\tau = \mu_t \frac{\partial u}{\partial z}$, there is

$$k = \frac{\tau}{\rho\sqrt{C_\mu}} \tag{10}$$

Based on the assumption that the shear stress gradient is constant along vertical direction, take derivatives for both sides of Eq. (10), then we get

$$\frac{\partial k}{\partial z} = \frac{1}{\rho\sqrt{C_\mu}}\frac{\partial \tau}{\partial z} = \text{const.} \tag{11}$$

Obviously, the TKE can be expressed by a first-order polynomial. Since the TKE decreases with the increase of roughness height $z_0$, the final expression of TKE is

$$k = Az + B \tag{12}$$

In which $A$ and $B$ are constants determined by fitting Eq.(12) to arbitrary measured or wind tunnel test data.

Therefore, by using logarithmic mean velocity profile Eq.(13) to describe the inflow velocity conditions, we can obtain the expression of ε showed in Eq.(14).

$$u = \frac{u_*}{\kappa}\ln\left(\frac{z + z_0}{z_0}\right) \tag{13}$$

$$\varepsilon = \frac{\sqrt{C_\mu}u_*}{\kappa(z + z_0)}(Az + B) \tag{14}$$

Moreover, the turbulent eddy viscosity in the SST k-ω model is given by $\mu_t = \frac{k}{\omega}$, thus, the specific dissipation rate can be described as

$$\omega = \frac{1}{C_\mu}\frac{\varepsilon}{k} = \frac{1}{\sqrt{C_\mu}}\frac{\partial u}{\partial z} = \frac{u_*}{\sqrt{C_\mu}\kappa(z + z_0)} \tag{15}$$

Thus, Eq.(12)~(15) compose the new inflow conditions based on the modified hypotheses in this paper.

### 2.3. Remedial approach for neutral equilibrium ABL

After applying the proposed inflow conditions as inlet boundary of an empty domain, we found that the mean velocity and TKE cannot maintain within the domain. The results can be found in section 4.1.1. Considering the efficiency and simplicity, we derive two kinds of remedial approaches to realize the consistence between inflow condition, boundary condition and wall treatment: 1) specify wall shear stress of the bottom boundary condition to matching the roughness of inflow conditions; 2) specify the values of inflow variables at first wall-adjacent layer grids to consider the error of the wall-function.

#### *2.3.1. Wall shear stress*

The turbulent HHABL flow satisfies the equilibrium condition. Figure 4 displays the force balancing of the whole flow field and it can be deduced that the flow field abides by the force balance condition

$$\tau_{top}L + F_1 H = \tau_{wall}L + F_2 H \tag{16}$$

In which $H$ is the height of the flow field and $L$ the length.

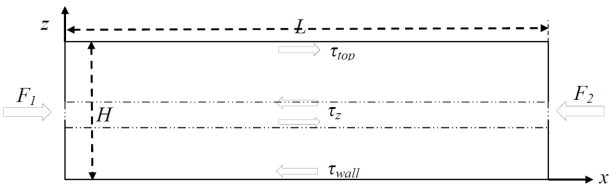



**Figure 4.** Sketch of force balancing of the flow field.

According to Eq.(16) and Eq.(11), there is

$$\frac{F_1-F_2}{L}=\frac{\tau_{top}-\tau_{wall}}{H}=\frac{\partial\tau}{\partial z}=\rho\sqrt{C_\mu}\frac{\partial k}{\partial z} \tag{17}$$

In which $\tau_{\text{top}}=\rho C_\mu\frac{k_{\text{top}}^2}{\varepsilon_{\text{top}}}\frac{\partial u}{\partial z}\Big|_{\text{top}}=\rho C_\mu\frac{u_*}{\kappa}\frac{k_{\text{top}}^2}{\varepsilon_{\text{top}}(H+z_0)}$ is the shear stress of top boundary and $H$ is the height of flow field.

Finally, the wall shear stress is:

$$\tau_{\text{wall}}=\tau_{\text{top}}-\rho\sqrt{C_\mu}H\frac{\partial k}{\partial z} \tag{18}$$

*2.3.2. Specific variable values in the wall-adjacent cells*

On the assumption that the inflow condition remains unchanged along the streamwise direction, specific TKE and TDR for the first wall-adjacent layer cells can be calculated. In the case of our new inflow condition, the specific variable values are determined with

$$k_{\text{sp}}=Az_{\text{sp}}+B \tag{19}$$

$$\varepsilon_{\text{sp}}=\frac{\sqrt{C_\mu}u_*}{\kappa(z_{\text{sp}}+z_0)}(Az_{\text{sp}}+B)\text{d} \tag{20}$$

In which $z_{\text{sp}}$ is the height of the cell centroid of the first wall-adjacent layer cells.

## 3. Numerical Setups

In this paper, the computational model simplifies the 3D model in Yang's work (Yang et al., 2009) to 2D plane model, and the results can verify the consistence of the 2D model with 3D model in simulations of turbulent HHABL. The computational domain is $L_x \times L_z =$ 12 m × 1.8 m in streamwise and vertical directions. The grids are

**Table 2.** Three Grid Schemes for HHABL simulation

| Parameters | $\Delta x$ (m) | $\Delta z_{wall}$(m) | Growth Factor | $N_x \times N_y$ |
|---|---|---|---|---|
| Coarse | 0.15 | 0.02 | 1.0987 | 80 × 35 |
| Medium | 0.10 | 0.01 | 1.0723 | 120 × 42 |
| Fine | 0.05 | 0.005 | 1.0321 | 240 × 65 |

**Table 3.** Computational Boundary Conditions for Simulations

| Domain boundary | Boundary conditions |
|---|---|
| Inlet | Velocity inlet: User Defined Functions with different inflow conditions |
| Outlet | Outflow: $\frac{\partial}{\partial x}(u,w,k,\varepsilon)=0$ |
| Top | Free-slip wall: $w=0,\frac{\partial}{\partial z}(u,k,\varepsilon)=0$ |
| Bottom | No-slip wall with enhanced wall treatment |

**Table 4.** Parameters for different TKE profiles

| TKE profiles | | K1 | K2 | K3 | K4 |
|---|---|---|---|---|---|
| Coefficient | $A$ | –0.3897 | –0.4081 | –0.5059 | –0.687 |
| | $B$ | 1.2517 | 0.9283 | 1.2063 | 1.296 |

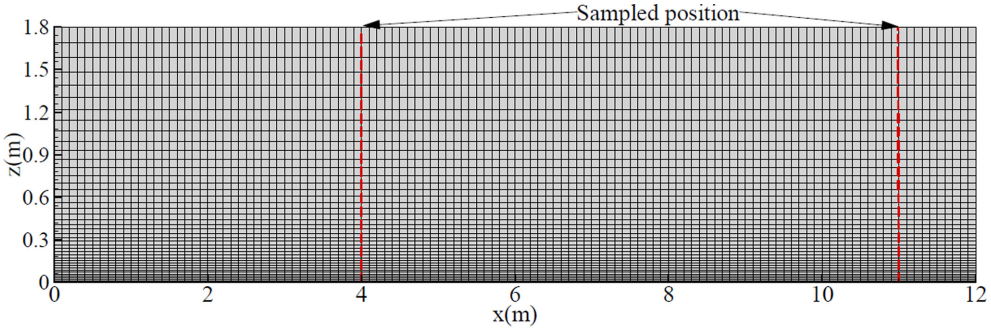
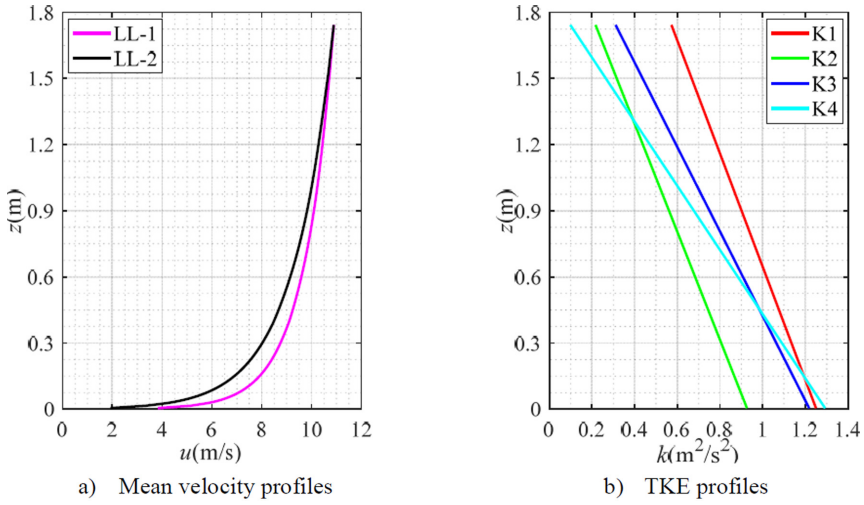



**Figure 5.** Computational domain and mesh scheme.

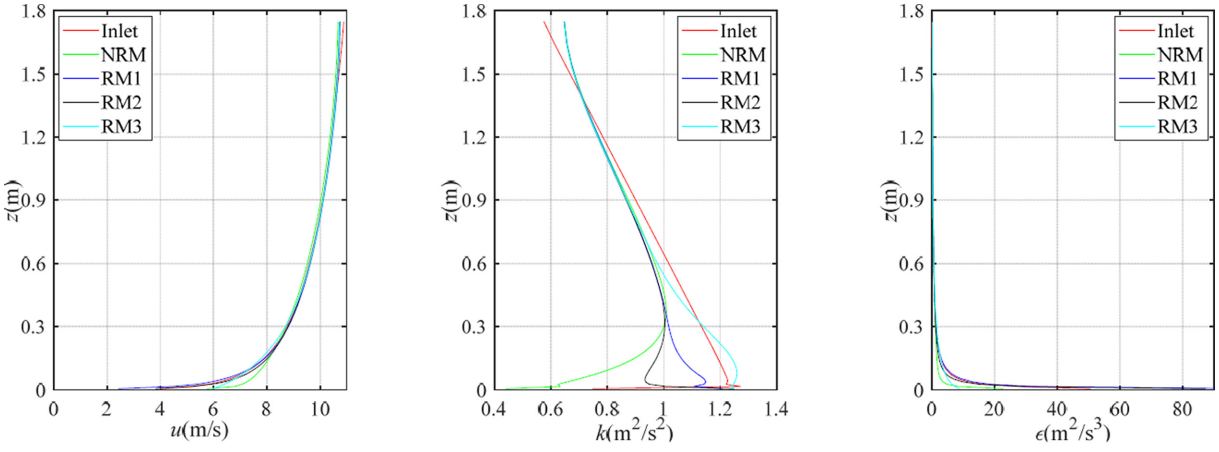
**Table 5.** Parameters for different inflow conditions

| Inflow conditions | | LIC-1 | LIC-2 | LIC-3 | LIC-4 | LIC-5 |
|---|---|---|---|---|---|---|
| Mean velocity profile | | LL-1 | LL-2 | | LL-1 | |
| TKE profile | | K1 | K1 | K2 | K3 | K4 |
| Remedy | $\tau_{\text{wall}}$ | 0.4600 | 0.2557 | 0.3411 | 0.4485 | 0.4763 |
| | $k_{\text{sp}}$ | 1.2497 | 1.2497 | 0.9262 | 1.2038 | 1.2926 |
| | $\varepsilon_{\text{sp}}$ | 87.3002 | 62.9159 | 64.7037 | 84.0920 | 90.2940 |
| | Reduced $\varepsilon_{\text{sp}}$ | 8.7300 | 6.2916 | 6.4704 | 8.4092 | 9.0294 |



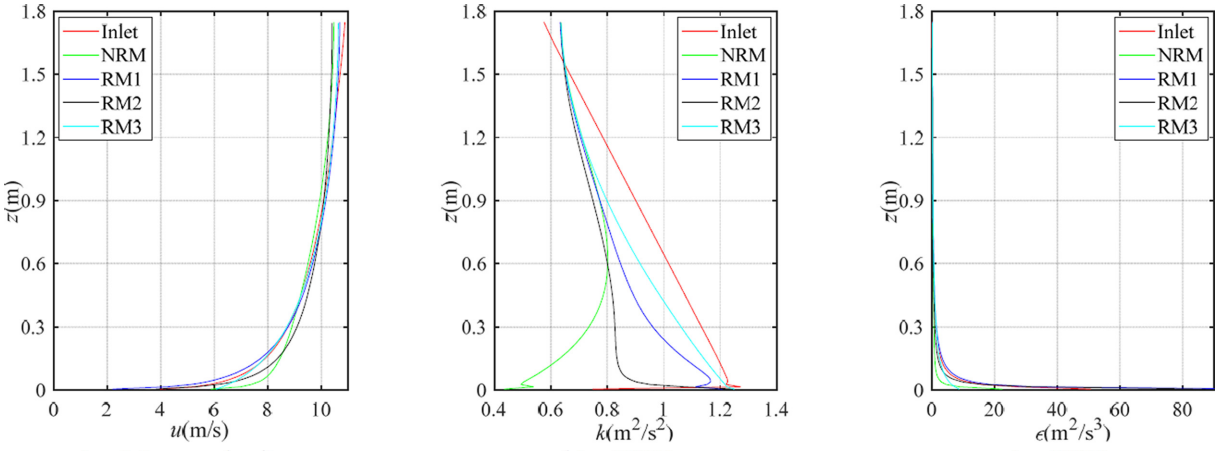

a) Mean velocity profiles b) TKE profiles

**Figure 6.** New inflow conditions.




a) Mean velocity b) TKE c) TDR

**Figure 7.** Comparison of LIC-1 results at $x_1$ with different remedies.




a) Mean velocity b) TKE c) TDR

**Figure 8.** Comparison of LIC-1 results at $x_2$ with different remedies.

uniformly distributed along x direction, and geometric expanded in vertical direction. As listed in Table 2, three uniformly distributed along x direction, and geometric expanded in vertical direction. As listed in Table 2, three grid schemes are used to test the grid-independence. The computational domain with medium grid scheme is showed in Figure 5. The two sampled positions are $x_1$ = 4 m and $x_2$ = 11 m.

All the simulations are performed with ANSYS-Fluent, and the boundary conditions are listed in Table 3. Since the roughness height is determined by $k_s = 9.793 z_0 / C_s$ (Blocken et al., 2007) with the constant $C_s = 0.5$, $z_0 = 2.25 \times 10^{-3}$m leads to $k_s = 0.0441$ m and the first layer grid height in current grid-scheme is 0.01 m < $2k_s$. So, the mesh scheme is incompatible with the standard wall function (Blocken et al., 2007; Gorlé et al., 2009) and we used enhanced wall-treatment (Kader, 1981) to release this restriction in following simulations. Compared to the standard wall function, which uses semi-empirical formulas to connect the viscosity-affected region between the wall

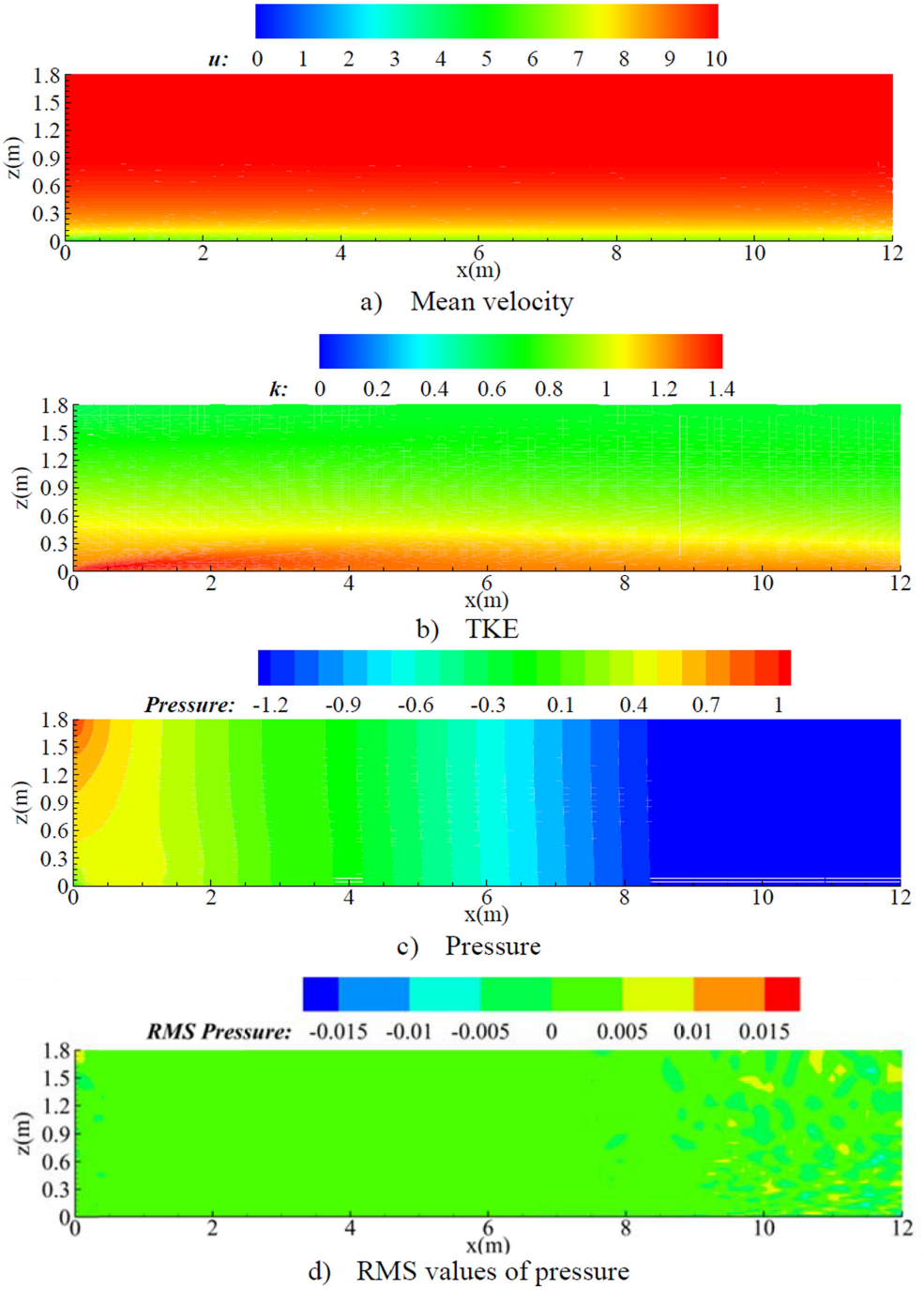



**Figure 9.** Contour of LIC-1 implemented with RM3.

and the fully-turbulent region, enhanced wall-treatment (EWT) is one of the near-wall modeling approaches that combines a two-layer model with enhanced wall functions to enable the viscosity-affected region be resolved all the way down to the wall. Thus, the turbulence closure that adopts EWT is more accurate, which requires a fine mesh resolution of the first layer grid adjacent to the wall.

The solution method is SIMPLEC algorithm of pressure-velocity coupling method and QUICK algorithm for the convection-diffusion equations. The residual convergence criteria for all variables are set as $10^{-6}$.

In this paper, two logarithmic mean velocity profiles with different roughness length, LL-1 with $z_0 = 2.25 \times 10^{-4}$m and LL-2 with $z_0 = 2.25 \times 10^{-3}$, with will be simulated. Besides, Table 4 lists the four types of TKE profiles, in which K1 is fitted according to wind tunnel test data, K2 profile is fitted according to wind tunnel test data (Gorlé et al., 2009), K3 profile is fitted according to Yang's TKE curve with $C_1 = -0.55$, $C_2 = 5.21$ (Yang et al., 2009) and K4 profile is referenced from Yan's work (Yan et al., 2015).

Table 5 lists five inflow conditions and corresponding remedial values. The wall shear stresses are calculated by Eq.(18), the specific TKE $k_{sp}$ and TDR $\varepsilon_{sp}$ in the first wall adjacent layer are calculated by substituting $z_{sp} = 0.005$ m into Eq.(19) and Eq.(20). All the TKE profiles and velocity profiles are plotted in Figure 6.

## 4. Results and Discussions

In this section, several cases for verifying the self-sustainability of the LIC inflow conditions with various TKE profiles, remedial approaches and standard k-ε turbulence model without changing the model constants are set. Firstly, we validate the remedial measures for LIC-1 and LIC-2 inflow conditions. Then the feasibility

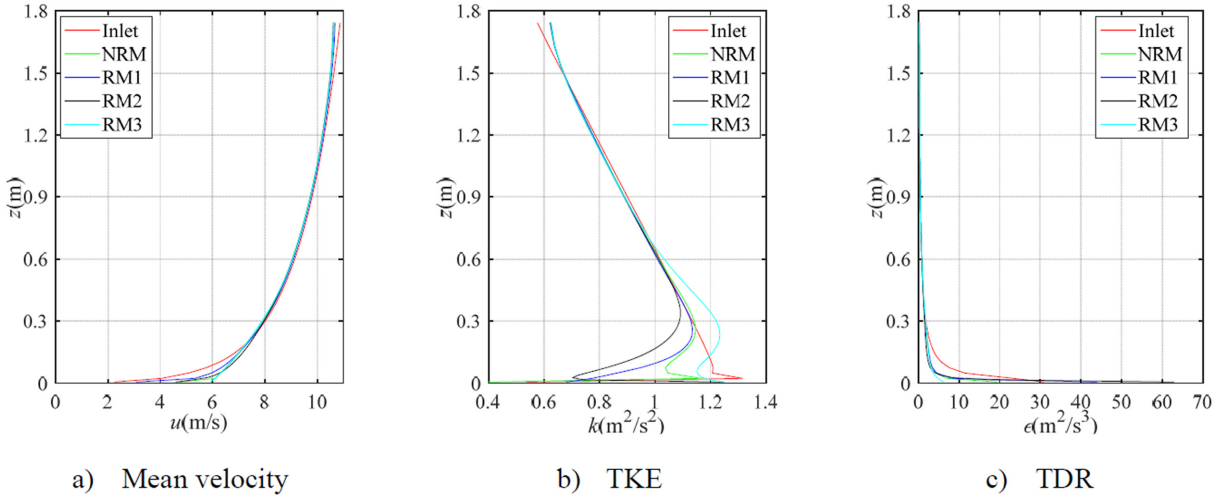



**Figure 10.** Comparison of LIC-2 results at $x_1$ with different remedies.

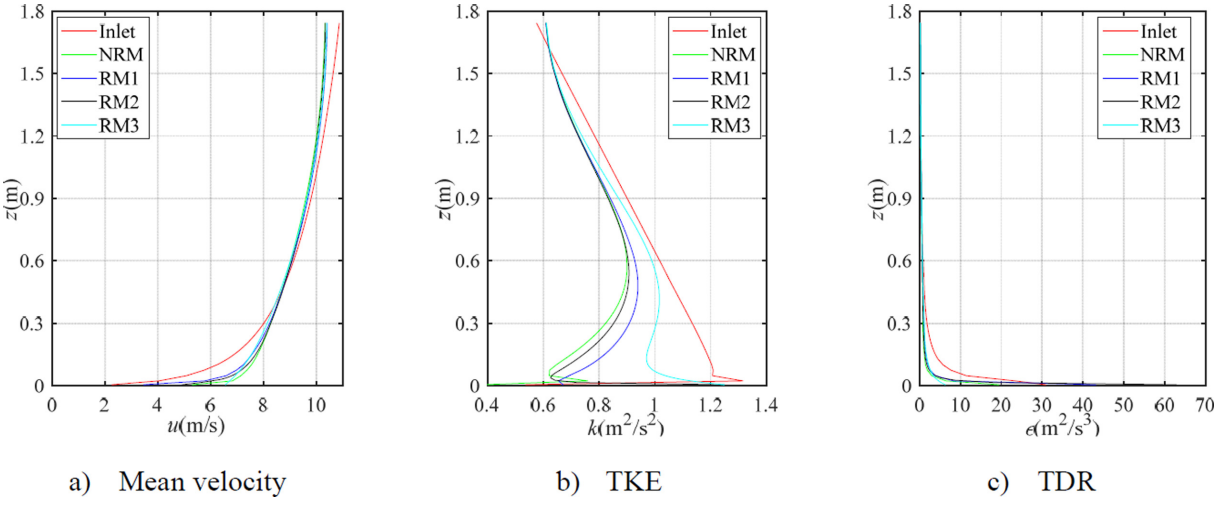



**Figure 11.** Comparison of LIC-2 results at $x_2$ with different remedies.

of the new type of inflow conditions and corresponding remedies are verified.

When comparing the results, NRM denotes the case without any remedial approaches, RM1 refers to case with adding wall shear stress, RM2 the case with specific $k_{sp}$ and $\varepsilon_{sp}$ in first wall adjacent layers and RM3 the case with wall shear stress, $k_{sp}$ and reduced $\varepsilon_{sp}$ in first wall adjacent cells.

### 4.1. Validation of the new inflow condition

#### *4.1.1. Inflow condition LIC-1*

Figure 7 and Figure 8 compare the mean velocity, TKE and TDR profiles at the two sampled positions. Apparently, the inflow properties in NRM cannot sustain through the domain and the deviation increase with stream-wise distance.

After adding the wall shear stress $\tau_{wall}$ in RM1 case, the

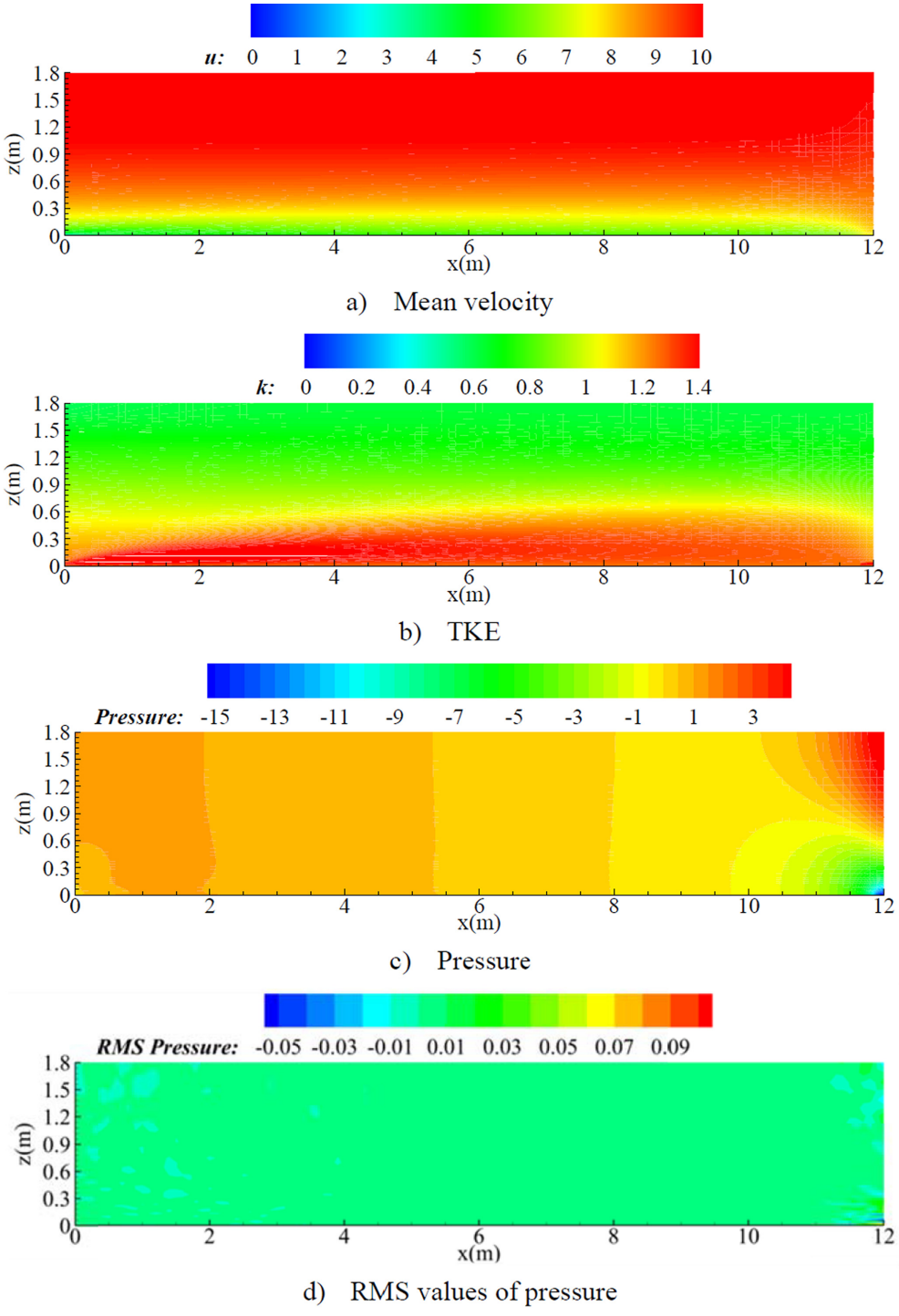



**Figure 12.** Contour of LIC-2 implemented with RM3.

mean velocity and TKE in near wall region are greatly improved. The downstream TDR is also larger than inflow value. Besides, specifying first wall-adjacent cell values by Eq.(19) and Eq.(20) in RM2 case, the results tell that although the TKE profiles maintains not well, the reduction trends are weakened and mean velocity in wall-adjacent layer sustains through the domain. Thus, combine RM1 with RM2 and reduce the TDR values in RM3 case, the TKE discrepancies are greatly mitigated, and the mean velocity is almost homogeneous through the domain. Furthermore, there exits errors at the top, which can be explained by the top boundary treatment and can be handled by the work of Cai (2014), Blocken (2007)and Hargreaves et al (2007).

In addition, without changing the turbulence model constants that usually determined by wind tunnel test, adding wall shear stress and specifying TKE and TDR values in first wall-adjacent layer cells, the proposed inflow conditions can reach to acceptable horizontal homogeneous state, also imply the simplicity and efficiency of this type of inflow conditions and corresponding remedial approaches.

Figure 9 shows the mean velocity, TKE and pressure contours of case LIC-1 implemented with RM3. The mean velocity contour depicts good homogeneous. Also, the pressure contour illustrates that the pressure changed linearly along flow direction and almost constant in vertical direction despite a slight variation near the inlet boundary, which can be explained by the transition from inflow data to the neutral boundary layer. The contour of root mean square (RMS) values of pressure in Figure 9 (d) also tells there is no obvious spurious pressure within the HHABL flow field under modification of RM3.

*4.1.2. Inflow condition LIC-2*

Figure 10 and Figure 11 compare the mean velocity, TKE and TDR profiles at two sampled positions. It is

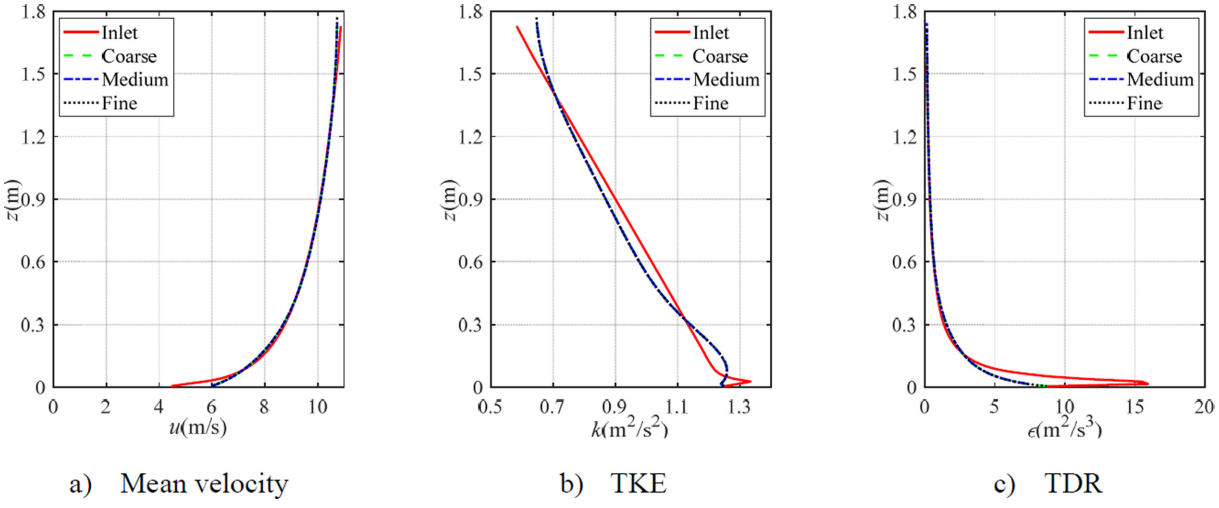



**Figure 13.** Comparison of LIC-1 inflow condition with three different grid schemes.

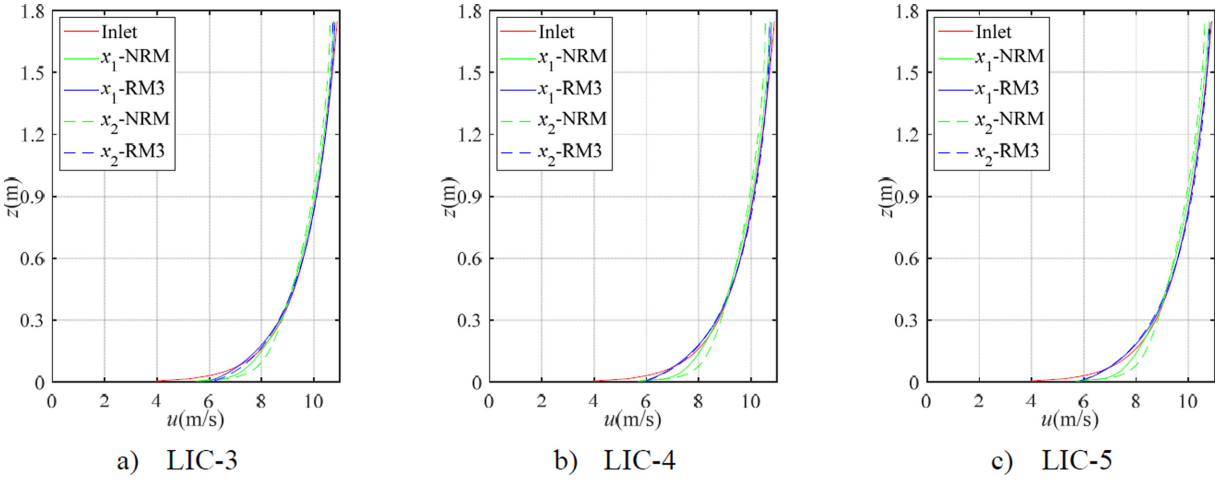



**Figure 14.** Mean velocity profiles of different inflow conditions.

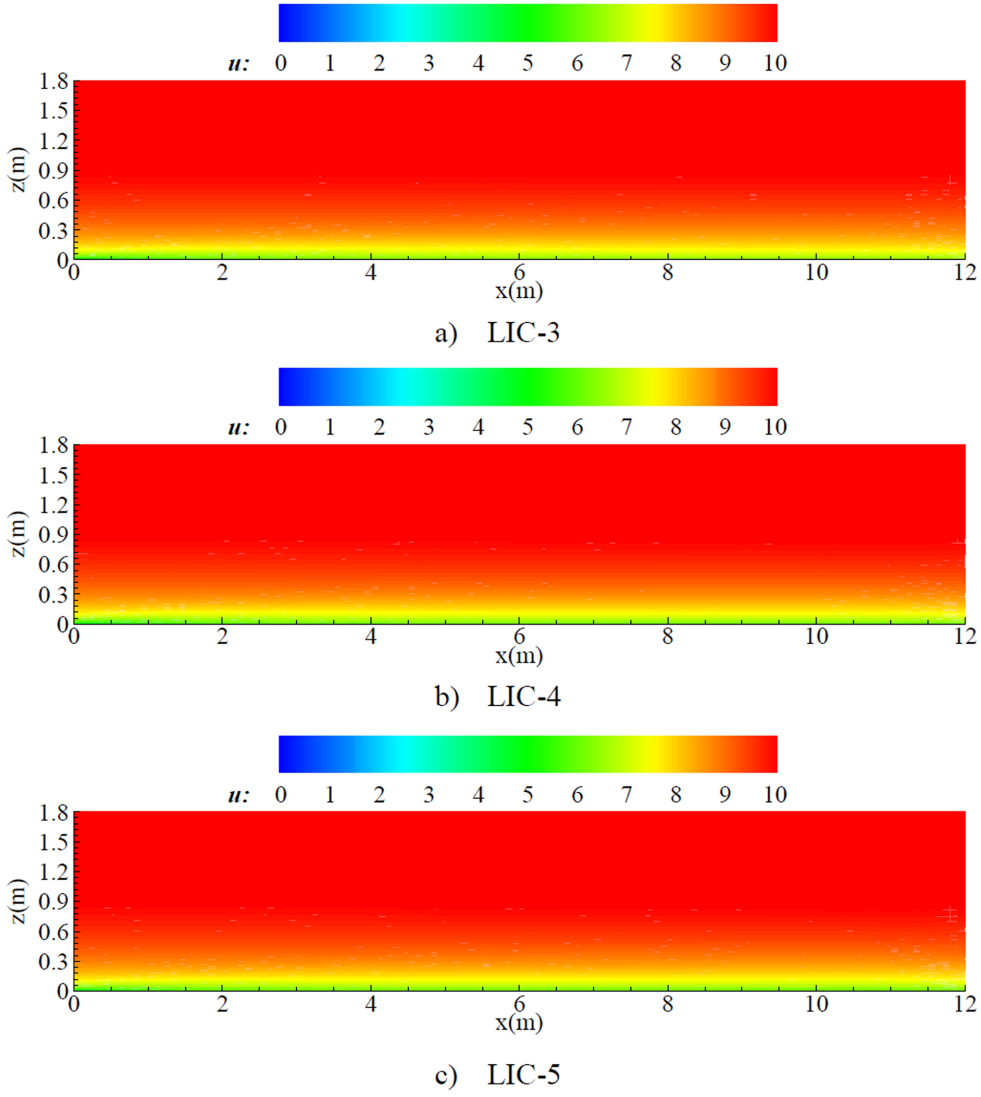



**Figure 15.** Contour of mean velocity for inflow conditions implemented with RM3.

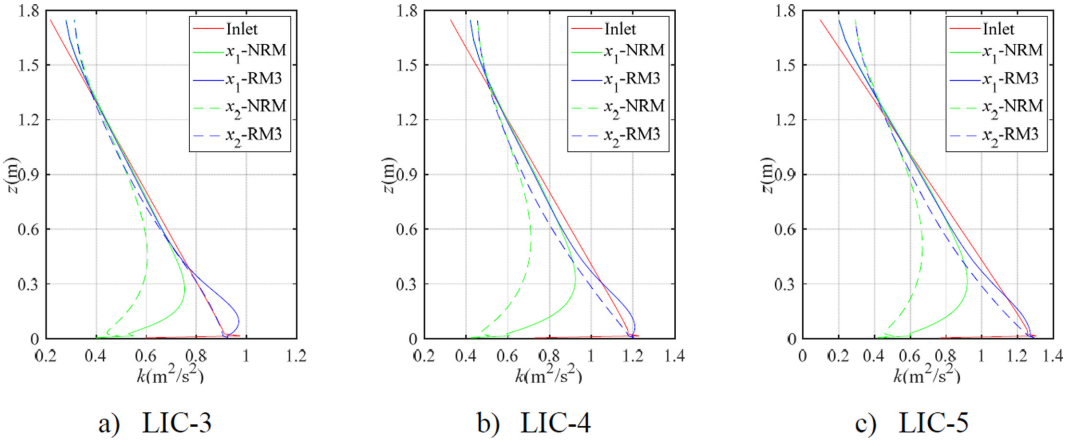



**Figure 16.** TKE profiles of different inflow conditions.

obvious that NRM case goes through a large reduction of mean velocity and TKE along flow direction. By specifying the TKE and TDR values for first wall cell and adding wall shear stress, the TKE discrepancies are efficiently lessened. However, the downstream mean velocity in near wall region, especially the wall adjacent layer, is

quite larger than inflow value. Figure 12 shows the contour of mean velocity, TKE and pressure of the RM3 case.

*4.1.3. Grid-independence analysis*

Numerical simulations for grid independence analysis are implemented based on inflow condition LIC-1 remedied with RM3. Figure 13 shows the mean velocity and TKE profiles at $x_1$. It can be observed that the numerical results are independent to grid scheme and the medium grid scheme gives adequate resolution for the simulations.

It should be noted that the inlet TKE calculated by Fluent has peaks at the second layer wall adjacent layer cells, which is a bit of different to the proposed linear Eq. (12) and cannot fixed by increasing grid resolution. This agrees with the results of Sumner et al (2012)that the peak is caused by the deviations introduced in numerical discretization process with standard finite volume methods.

**4.2. Application to different linear TKE inflow conditions**

Figure 14 displays the mean velocity profiles simulated with inflow conditions LIC-3, LIC-4 and LIC-5, Figure 15 depicts the mean velocity contour of the three cases. It can be seen that the mean velocity can maintain well through domain, this illustrates that both inflow conditions can reach to equilibrium profiles with additional remedial measure RM3.Figure 16

Figure 16 depicts the TKE profiles simulated with inflow conditions LIC-3, LIC-4 and LIC-5, Figure 17 gives the TKE contour of the three cases. Same with LIC-1, although the TKE slightly attenuated along the flow direction, the reduction is greatly weakened by using additional remedial measure RM3.

Figure 18 shows the pressure contour of the three cases, both of which tells that the pressure changes linearly along flow direction and keep constant along vertical direction. The corresponding RMS values of pressure contours are also displayed in Figure 19, which tell that there is no spurious pressure within the obtained HHABL flow field.

To sum up, by applying the remedial approaches, adding wall shear stresses, and specifying the variable values of

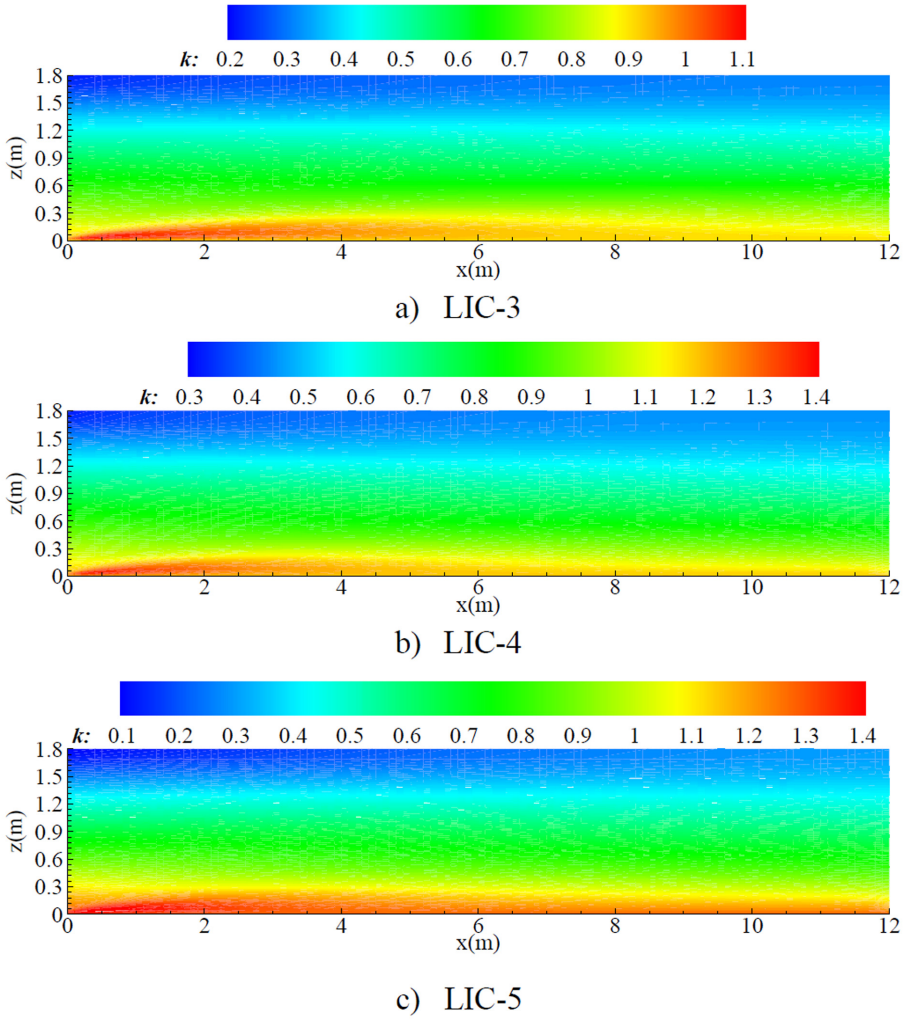



**Figure 17.** Contour of TKE for inflow conditions implemented with RM3.

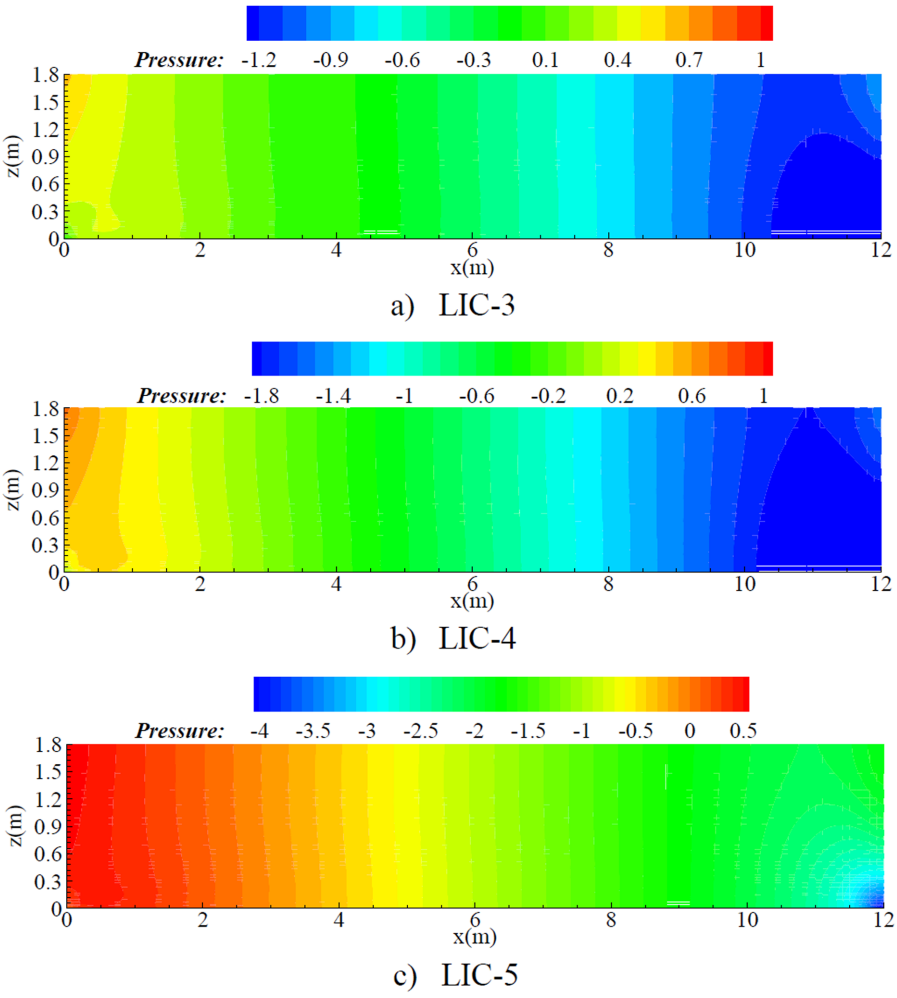



**Figure 18.** Contour of pressure for inflow conditions implemented with RM3.

first wall adjacent layer to three sets of inflow conditions, we verify the feasibility of inflow conditions proposed in this paper and the capability of the remedial approach in reducing the streamwise gradients of mean velocity and TKE.

## 5. Concluding remarks

By analyzing the previous CFD modeling turbulent HHABL results, we found that the existed pressure gradient is close to the shear stress vertical gradient, but both are not zeros, which is not in consistence with their pre-hypotheses. According to this conclusion, in this paper we modify the past hypotheses and then detailed derive a new type of inflow condition for standard k-ε turbulence model. Besides, by fitting the existing inflow conditions, we give four TKE profiles of the inflow condition.

To obtain horizontally homogeneous, neutral stratified ABL, we derive a group of remedial approach, which including a formulation for wall shear stress and fixing the values of TKE and TDR in first wall adjacent layer cells for the linear TKE profiles and logarithmic mean velocity profiles. By comparing the remedial approaches, it is found that the combination of wall shear stress and specific TKE and TDR values in the first wall adjacent layer is simple and effective for modeling turbulent HHABL for there is no extra needs to determining the turbulence model constants. And this kind of approach is feasible and valid for different type of inflow condition including linear TKE profiles.

Furthermore, it should be noticed that for the inflow condition with relatively large roughness height $z_0$, the optimal remedial measure cannot obtain well maintained ABLs, especially for the mean velocity. This may be attributed to the wall-function problems and also a potential problem needed to be further studied.

## Acknowledgements

This research has received support from the Shenzhen Knowledge Innovation Program (No. JCYJ20190806145216643) and the National Natural Science Foundation of China (51778200), all of which are gratefully acknowledged.

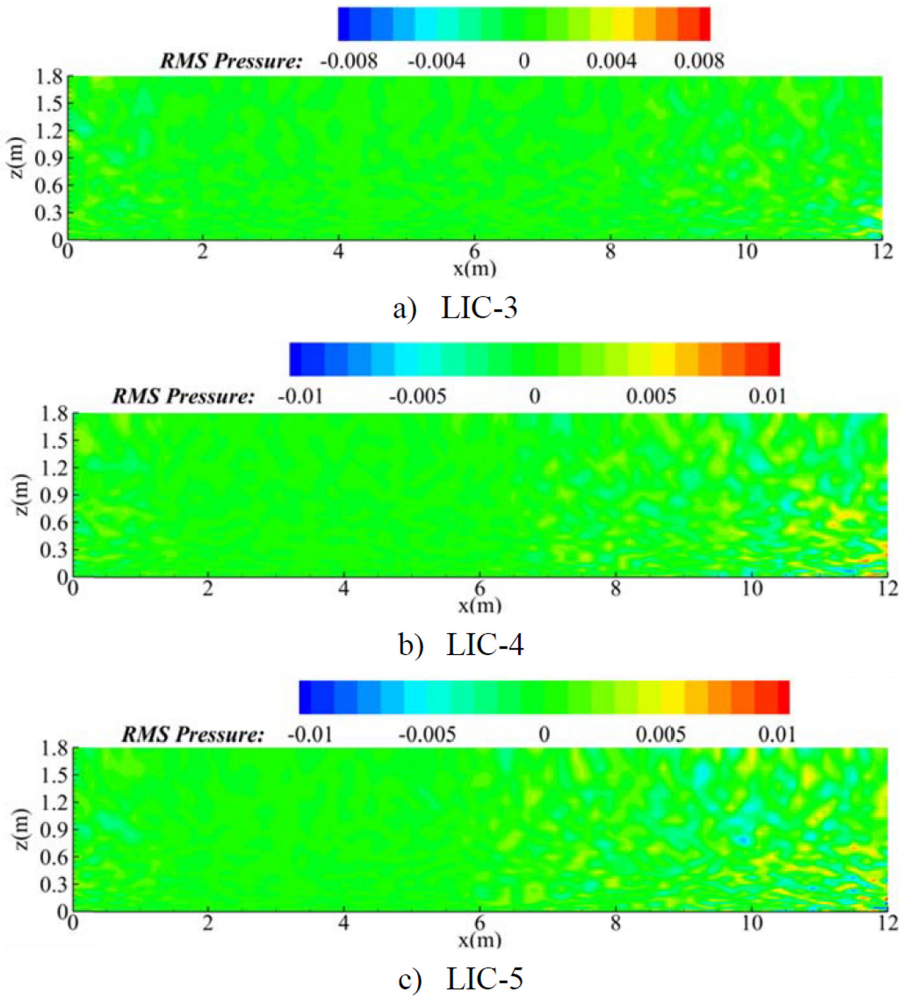



**Figure 19.** Contour of RMS pressure for inflow conditions implemented with RM3

## References


Balogh, M., Parente, A., 2015. Realistic boundary conditions for the simulation of atmospheric boundary layer flows using an improved k-ε model. J. Wind Eng. Ind. Aerod. 144, 183-190.

Balogh, M., Parente, A., Benocci, C., 2012. RANS simulation of ABL flow over complex terrains applying an Enhanced k-ε model and wall function formulation: Implementation and comparison for fluent and OpenFOAM. J. Wind Eng. Ind. Aerod. 104-106, 360-368.

Blocken, B., Carmeliet, J., Stathopoulos, T., 2007. CFD evaluation of wind speed conditions in passages between parallel buildings-effect of wall-function roughness modifications for the atmospheric boundary layer flow. J. Wind Eng. Ind. Aerod. 95, 941-962.

Blocken, B., Stathopoulos, T., Carmeliet, J., 2007. CFD simulation of the atmospheric boundary layer: wall function problems. Atmos. Environ. 41, 238-252.

Blocken, B., Stathopoulos, T., van Beeck, J.P.A.J., 2016. Pedestrian-level wind conditions around buildings: Review of wind-tunnel and CFD techniques and their accuracy for wind comfort assessment. Build. Environ. 100, 50-81.

Cai, X., Huo, Q., Kang, L., Song, Y., 2014. Equilibrium Atmospheric Boundary-Layer Flow: Computational Fluid Dynamics Simulation with Balanced Forces. Bound.-Lay. Meteorol. 152, 349-366.

Gorlé, C., van Beeck, J., Rambaud, P., Van Tendeloo, G., 2009. CFD modelling of small particle dispersion: The influence of the turbulence kinetic energy in the atmospheric boundary layer. Atmos. Environ. 43, 673-681.

Hargreaves, D.M., Wright, N.G., 2007. On the use of the k-model in commercial CFD software to model the neutral atmospheric boundary layer. J. Wind Eng. Ind. Aerod. 95, 355-369.

Hu, P., Li, Y., Cai, C.S., Liao, H., Xu, G.J., 2013. Numerical simulation of the neutral equilibrium atmospheric boundary layer using the SST k-ω turbulence model. Wind Struct. 17, 87-105.

Jones, W.P., Launder, B.E., 1972. The prediction of laminarization with a two-equation model of turbulence. Int. J. Heat Mass Tran. 15, 301-314.

Juretić, F., Kozmar, H., 2013. Computational modeling of the neutrally stratified atmospheric boundary layer flow using the standard k-ε turbulence model. J. Wind Eng. Ind. Aerod. 115, 112-120.

Juretić, F., Kozmar, H., 2014. Computational modeling of the atmospheric boundary layer using various two-equation turbulence models. Wind Struct. 19, 687-708.

Kader, B.A., 1981. Temperature and concentration profiles in fully turbulent boundary layers. Int. J. Heat Mass Tran. 24, 1541-1544.

Launder, B.E., Spalding, D.B., 1974. The numerical computation of turbulent flows. Comput. Method. Appl. M. 3, 269-289.

Longo, R., Ferrarotti, M., Sánchez, C.G., Derudi, M., Parente, A., 2017. Advanced turbulence models and boundary conditions for flows around different configurations of ground-mounted buildings. J. Wind Eng. Ind. Aerod. 167, 160-182.

O' Sullivan, J.P., Archer, R.A., Flay, R.G.J., 2011. Consistent boundary conditions for flows within the atmospheric boundary layer. J. Wind Eng. Ind. Aerod. 99, 65-77.

Parente, A., Gorlé, C., van Beeck, J., Benocci, C., 2011a. A Comprehensive Modelling Approach for the Neutral Atmospheric Boundary Layer: Consistent Inflow Conditions, Wall Function and Turbulence Model. Bound.-Lay. Meteorol. 140, 411-428.

Parente, A., Gorlé, C., van Beeck, J., Benocci, C., 2011b. Improved k-ε model and wall function formulation for the RANS simulation of ABL flows. J. Wind Eng. Ind. Aerod. 99, 267-278.

Peralta, C., Nugusse, H., Kokilavani, S.P., Schmidt, J., Stoevesandt, B., 2014. Validation of the simpleFoam (RANS) solver for the atmospheric boundary layer in complex terrain. EDP Sciences,

Richards, P.J., Hoxey, R.P., 1993. Appropriate Engineering Boundary Conditions For Computational Wind Models Using The k-ε Turbulence Model. J. Wind Eng. Ind. Aerod. 145-153.

Richards, P.J., Norris, S.E., 2011. Appropriate boundary conditions for computational wind engineering models revisited. J. Wind Eng. Ind. Aerod. 99, 257-266.

Richards, P.J., Norris, S.E., 2015. Appropriate boundary conditions for a pressure driven boundary layer. J. Wind Eng. Ind. Aerod. 142, 43-52.

Riddle, A., Carruthers, D., Sharpe, A., McHugh, C., Stocker, J., 2004. Comparisons between FLUENT and ADMS for atmospheric dispersion modelling. Atmos. Environ. 38, 1029-1038.

Sumner, J., Masson, C., 2012. k-ε simulations of the neutral atmospheric boundary layer: analysis and correction of discretization errors on practical grids. Int. J. Numer. Meth. Fl. 70, 724-741.

Wilcox, D.C., 1998. Turbulence modeling for CFD. DCW industries La Canada, CA,

Yan, B.W., Li, Q.S., He, Y.C., Chan, P.W., 2015. RANS simulation of neutral atmospheric boundary layer flows over complex terrain by proper imposition of boundary conditions and modification on the k-ε model. Environ. Fluid Mech. 16, 1-23.

Yang, W., Quan, Y., Jin, X., Tamura, Y., Gu, M., 2008. Influences of equilibrium atmosphere boundary layer and turbulence parameter on wind loads of low-rise buildings. J. Wind Eng. Ind. Aerod. 96, 2080-2092.

Yang, Y., Gu, M., Chen, S., Jin, X., 2009. New inflow boundary conditions for modelling the neutral equilibrium atmospheric boundary layer in computational wind engineering. J. Wind Eng. Ind. Aerod. 97, 88-95.

Yang, Y., Xie, Z., Gu, M., 2017. Consistent inflow boundary conditions for modelling the neutral equilibrium atmospheric boundary layer for the SST k-omega model. Wind Struct. 24, 465-480.

Yu, H., Thé, J., 2017. Simulation of gaseous pollutant dispersion around an isolated building using the k-ω SST (shear stress transport) turbulence model. J. Air Waste Manage. 67, 517-536.